Appl. Phys. A (2017) 123:659
DOI 10.1007/s00339-017-1267-9

Applied Physics A
Materials Science & Processing



RAPID COMMUNICATION

# Nanostructured tetragonal barium titanate produced by the polyol and spark plasma sintering (SPS) route

**Ulises Acevedo-Salas[1] · Romain Breitwieser[2] · Thomas Gaudisson[2] · Sophie Nowak[2] · Souad Ammar[2] · Raúl Valenzuela[1]**

Received: 16 February 2017 / Accepted: 19 September 2017 / Published online: 22 September 2017


**Abstract** There is a great interest to synthesize ferroelectric ceramics both with fine grain size and significant electric properties. Here, we report the preparation of nanostructured tetragonal barium titanate by combining forced hydrolysis of metallic salts in polyol, soft annealing and 650 °C spark plasma sintering under uniaxial pressure of 120 MPa for 5 min. The stabilization of highly dense (density of 90%), nanostructured (grains about 50 nm) tetragonal barium titanate ceramic was achieved. The produced ceramic exhibited ferroelectric behavior and a dielectric permittivity of 3600 at 1 kHz and room temperature.

## 1 Introduction

Barium titanate $BaTiO_3$ (BTO) has attracted great attention in a wide range of high technological applications [1]. It is usually prepared by conventional solid-state techniques, which are associated with unavoidable drawbacks such as high calcination temperatures (> 1000 °C), time and energy consumption. Conventional methods lead to large grains, unsuitable to fulfill the growing demand of nanostructured BTO bodies for electronic devices.

The synthesis of nanosized BTO can lead to a strong decrease in permittivity due to the partial or total transition from the tetragonal (ferroelectric) to the cubic (paraelectric) phase [2]. This phenomenon is due to surface effects, as well as to the crystal quality of the obtained grains [3]. Many efforts to stabilize the tetragonal BTO phase on nanoparticles have been carried out by different methods such as microwave synthesis [4], solvothermal methods [5], and soft chemistry [6].

To produce nanostructured functional solids, the combination of soft chemistry followed by spark plasma sintering (SPS) is relatively new, but it is currently the only technique preserving final grain size within nanosize range. In the SPS process, the starting powder is pressed in a graphite die by two pistons at pressures up to 120 MPa, under vacuum. Electric pulses heat the conductive die, allowing very rapid heating and cooling rates (1000 °C/min). Diffusion in the sample is significantly enhanced by the current pulses, or the electric field in insulating samples [7], and high densities can be reached at very low temperatures and extremely short times, preserving a grain size in the nanometric range.

Some attempts have been made to consolidate nanograined BTO by means of SPS at temperatures higher than 800 °C starting from nanosized powders. However, critical size effects on dielectric and ferroelectric properties were observed and evidenced by a pronounced drop on dielectric constant, for ceramics with grain sizes below 500 nm [8] (relative permittivity values near 700 at $10^4$ Hz for a 50 nm grain-sized sample). These findings were attributed to the presence of a cubic and non-ferroelectric dead layer at the grain boundaries. Nonetheless, a complete study of size effects on the structure of BTO ceramics was reported in [9]. Ferroelectricity was proven for a 20-nm grain-sized sample as well as the coexistence of different Raman active

✉ Raúl Valenzuela
monjaras@unam.mx

[1] Instituto de Investigaciones en Materiales, Universidad Nacional Autónoma de México, P.O. Box 70-360, 04510 Coyoacán, Ciudad de México, Mexico

[2] ITODYS, Université Paris Diderot, PRES Sorbonne Paris Cité, CNRS UMR-7086, 15, Rue Jean Antoine de Baïf, 75205 Paris, France

symmetries, such as orthorhombic/rhombohedral at low temperatures and tetragonal/distorted-cubic above room temperature. Such structures can be associated with good dielectric and ferroelectric properties.

In this manuscript, we describe the synthesis of BTO ceramics by means of the polyol process [10] followed by SPS at 650 °C. To the best of our knowledge, the use of polyol-synthesized precursors for SPS consolidation in BTO has been never reported previously. We show that this combination of techniques led to the stabilization of a proven ferroelectric-nanostructured BTO with high dielectric constant values (around 3600 for the relative real part at 1 kHz). We ascribe these results to the presence of a tetragonal phase on our samples which is probably coexisting with a distorted-cubic and thus, ferroelectric phase at grain boundaries.

## 2 Materials and methods

### 2.1 Synthesis

Barium (II) acetate (Johnson Matthey *Alfa* Products, reagent grade purity) and titanium (IV) isopropoxide (Acros Organics, $\geq$ 98% purity) were dissolved in 0.9875 L of diethylen eglycol (Acros Organics, $>$ 99% purity), in the stoichiometric ratio. The mixture was brought to 145 °C under mechanical stirring until the dissolution of the metal precursors. Sodium hydroxide (micropearls for analysis from Acros Organics) was then added and the total mixture was brought to the boiling point (229 °C) at a 6 °C/min heating rate, maintained in reflux and stirring for 3 h. After cooling, the precipitated solid was recuperated by centrifugation, washed with ethanol then water, three times, and dried in air at 50 °C overnight. The recovered powder was pre-treated in air (Fig. 1 left). The best temperature for the formation of $BaTiO_3$ phase was 650 °C, however, some traces of barium carbonate was still present. The powder was thus calcined at 650 °C for 2, 6 and 8 h to achieve the complete formation of the titanate and eliminate the carbonate (Fig. 1 right). The quantity of carbonate was reduced below 2% after 8 h of calcination. The SPS process was carried out in a DR. SINTER515S SYNTEX SPS machine (Thiais, France). A heating rate of 38 °C/min was used. To eliminate organic remains of the reaction, a first plateau at 280 °C for 10 min was applied. The temperature was then increased to the 500–900 °C range, increasing also the pressure from its initial value (50) to 120 MPa. The sintering time was 5 min. The best results were obtained at 650 °C; at 900 °C the partial formation of a reduced secondary crystalline phase $BaTi_2O_5$ was observed. At 500 °C, a good crystalline phase was obtained but mechanical properties were poor. The pressure of 120 MPa was selected because it is the higher pressure which can be applied to the graphite die without breaking (at 650 °C).

### 2.2 Characterization

The X-ray diffraction (XRD) patterns of powders and pellets (Figs. 1, 3) were recorded using a Panalytical X'Pert Pro diffractometer at Co-K$\alpha$ radiation (K$\alpha$ = 1.79031 Å) equipped with a multichannel detector X'celerator, in the $\theta$–$\theta$ Bragg–Brentano geometry (0.025° for 2 s). Temperature-resolved XRD patterns were recorded from 25 to 900 °C (50 °C steps, see Fig. 1 left). The high temperature oven chamber is an Anton Paar HTK 1200 N and to obtain an inert atmosphere, we used a nitrogen flux. The cell parameters and the size of crystallites were determined by means of the MAUD software [11]. Polycrystalline strain-free silicon was used as the standard to quantify the instrumental peak's broadening contribution. The microstructure was studied by scanning electron microscopy (SEM) using a Supra 40 ZEISS FEG-SEM microscope operating at 5.0 kV. Density was measured with a Micrometrics AccuPyc 1330 helium pycnometer. Raman scattering spectroscopy was performed with a Jobin–Yvon U1000 double monochromator spectrophotometer, with a 514.5 nm line from a Spectra-Physics 2020 argon-ion laser at 10 mW. Three measured Raman spectra were averaged. Commercial BTO (Fluka Chemika, purity 99.9%) was used as a reference. Electrical permittivity was measured on pellets with gold electrodes, with an impedance analyzer HP 4192A in the 5–13 MHz frequency range. Polarization curves were also measured as function of the applied electric field with a RADIANT Tech. Inc. Precision RT66B polarizer, working up to 4 kV.

## 3 Results and discussion

### 3.1 Phase analysis

FEG-SEM micrographs showed homogeneously sized and shaped grains ranging down to 50 nm (Fig. 2). The XRD pattern of the BTO pellet sintered at 650 °C is shown in Fig. 3. Focusing on the (200) reflection line, an unusual broadening can be observed compared with other peaks. This broadening is associated with the splitting of (200) and (002) reflections coming from grains with a high fraction of tetragonal symmetry [12, 13]. It is important to point out that all the observed peaks present high broadening contributions coming from nanosized coherent diffraction domains (or crystallites). The calculated crystallite size from the corresponding refinement is $L_{XRD} = 48$ nm which matches well with grain sizes

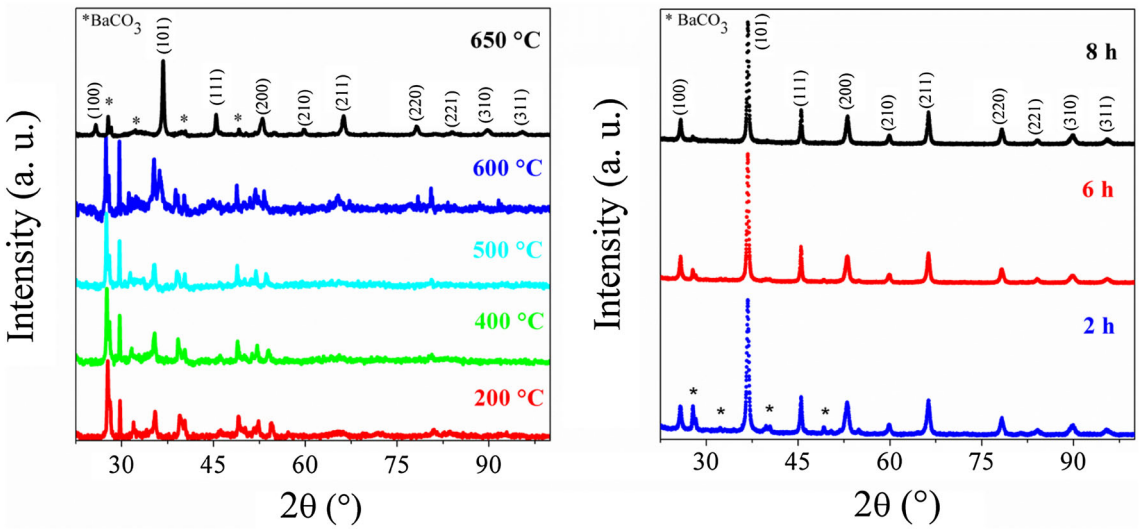


**Fig. 1** Left: Temperature-resolved XRD patterns of polyol-synthesized sample; right: XRD patterns of the powder calcined at 650 °C during 2, 6 and 8 h

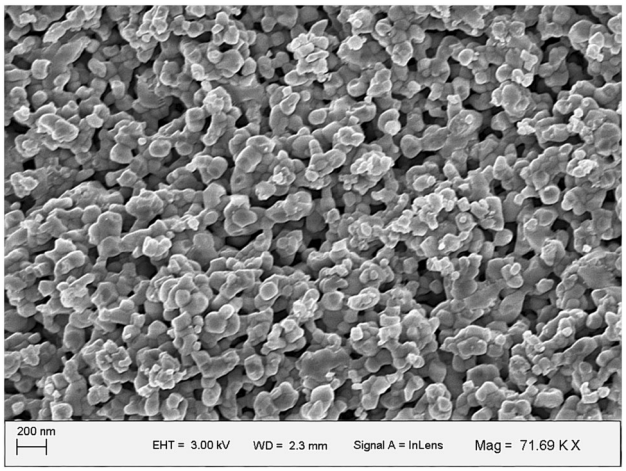


**Fig. 2** SEM micrograph of the consolidated sample

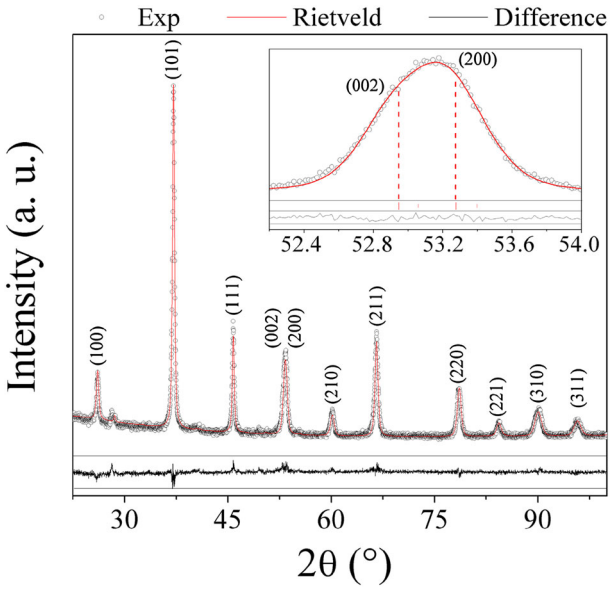


**Fig. 3** Experimental and MAUD-refined XRD pattern of the SPS consolidated sample; inset: MAUD refinement of 002/200 diffracted peak

observed in Fig. 2. This feature, combined with the splitting of (200) and (002) reflections causes the formation of a single unusual broadened peak near 53° (2$\theta$). A detailed MAUD refining between 52 and 54° (2$\theta$) was performed (using ICSD no° 248395), leading to a good agreement with the tetragonal structure as illustrated by the quality fit (sig factor = 1.9 and rw = 5.1) in Fig. 3 (inset). The refined cell parameters are $a = 3.993$ (2) and $c = 4.016$ (2), which agree very well with tetragonal BTO ($c/a = 1.006$).

Raman spectrum was recorded and compared to that of commercial tetragonal BTO (Fig. 4 left). A good agreement of all the samples is clearly noticed. Raman absorptions at $\sim$ 180, 270, 308 and 520 $cm^{-1}$ accurately fit with $1A_1$(TO), $2A_1$(TO), E(TO) and $3A_1$(TO) transverse optical modes, respectively, as reported for tetragonal BTO [14].

In contrast, the longitudinal optical mode $A_1$(LO) observed at 715 $cm^{-1}$ for the reference, and previously reported for nanostructured BTO systems [12, 15] are absent in our samples. The vanishing of these modes has been observed in some BTO thin films. It was attributed to light scattering from domain walls [16]. The same effect was observed in single crystals when the incident light was parallel to the polarization vector, and the laser beam cross-section matched ferroelectric single domains [17]. Such correlation could, therefore, explain the absent lines in our samples, if we assume that both calcined particles and sintered grains are small enough to contain single domains.

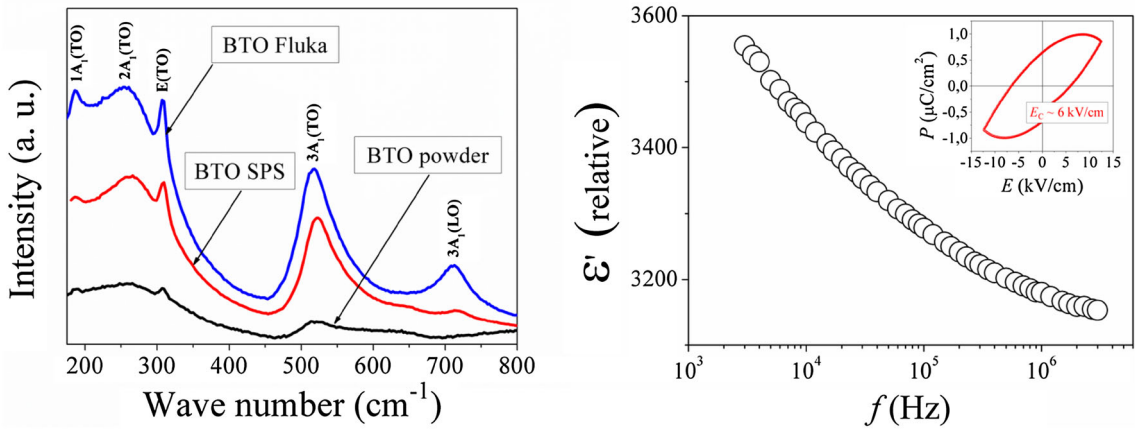


**Fig. 4** Left: Raman spectra of polyol and SPS samples compared with commercial BTO; right: electrical permittivity as a function of frequency and ferroelectric hysteresis loop for consolidated pellet (inset)

### 3.2 Dielectric characterization

The real part of the dielectric constant (Fig. 4, right) showed a relative $\varepsilon'$ at 1 kHz around 3600, a similar value to that reported for nanostructured BTO in [18] but higher than those in [8]. In addition, a ferroelectric hysteresis loop can be well distinguished on the polarization curve shown in Fig. 4 (right, inset), regardless of some losses that can be also observed (round-shaped and non-saturated at high fields). The latter proves that a ferroelectric behavior is present on our samples and, based on these features, the existence of a non-ferroelectric dead layer lying at the boundaries can not be assumed accurately. Moreover, it has been found that grain boundaries in BTO may well contain a ferroelectric phase, similar to ferroelectric grains [19] (probably a distorted-cubic phase as that proposed in [9]). All these results guided us, therefore, to assume a high fraction of tetragonal BTO within grains stabilized in our samples, probably coexisting with a distorted and thus, ferroelectric, cubic phase at the boundaries.

## 4 Conclusions

A high density BTO body was obtained by a combination of polyol process and SPS technique, at low sintering temperature and very short time (650 °C for 5 min) under a uniaxial pressure of 120 MPa. The as-obtained studied sample exhibited grain sizes ranging down to 50 nm, a high dielectric constant and proven ferroelectric behavior. XRD and Raman spectroscopy confirmed that a high fraction of stable tetragonal BTO constituted the produced nanostructured ceramic. The Raman spectra suggested a ferroelectric single-domain behavior. Additionally, the presence of a distorted-cubic ferroelectric phase at boundaries is proposed to explain the high permittivity values and ferroelectric behavior exhibited by this sample.

**Acknowledgements** This work was supported by the French Ministry of Research and National Center for Scientific Research. ANR (Agence Nationale de la Recherche) and CGI (Commissariat à l'Investissement d'Avenir) are gratefully acknowledged for their financial support of this work through the Science and Engineering for Advanced Materials and devices (SEAM) Labex, ANR 11 LABX 086, ANR 11 IDEX 05 02.

## References

1. L.G. Tejuca, J.L.G. Fierro, *Properties and applications of perovskite-type oxides* (Marcel Dekker Inc., New-York, 1993)
2. A. Vlad Zanfir, G. Voicu, S. Ion Jinga, E. Vasile and V. Ionita, Low temperature synthesis of barium titanate nanopowders. Ceram. Int. **42**, 1672–1678 (2016)
3. V.V. Laguta, C. Elissalde, M. Maglione, A.M. Artemenko, V. Chlan, H. Štěpánková, Yu. Zagorodniy, Crystal structure transformation induced by surface stresses in $BaTiO_3$ and $BaTiO_3$@$SiO_2$ nanoparticles and ceramics. Phase Transf. **88**, 761–775 (2015)
4. H. Takahashi, Y. Numamoto, J. Tani, S. Tsurekawa, Considerations for $BaTiO_3$ ceramics with high piezoelectric properties fabricated by microwave sintering method. Jpn. J. Appl. Phys. **47**, 8468–8471 (2008)
5. H.C. Du, S. Wohlrab, M. Weiß, S. Kaskel, Preparation of $BaTiO_3$ nanocrystals using a two-phase solvothermal method. J. Mater. Chem. **17**, 4605–4610 (2007)
6. M. Niederberger, N. Pinna, J. Polleux, M.R. Antonietti, A general soft chemistry route to perovskites and related materials: synthesis of $BaTiO_3$, $BaZrO_3$ and $LiNbO_3$ nanoparticles. Angew. Chem. Int. Ed. **43**, 2270–2273 (2004)
7. O. Guillon, J. Gonzalez-Julian, B. Dargatz, T. Kessel, G. Schierning, J. Rathel, M. Hermann, Field-assisted sintering technology/spark plasma sintering: mechanisms, materials, and technology developments. Adv. Eng. Mater. **16**, 830–849 (2014)
8. Z. Zhao, V. Buscaglia, M. Viviani, M.T. Buscaglia, L. Mitoseriu, A. Testino, M. Nygren, M. Johnsson, P. Nanni, Grain-size effects on the ferroelectric behavior of dense nanocrystalline $BaTiO_3$ ceramics. Phys. Rev. B **70**, 024107 (2004)

9. X. Deng, X. Wang, H. Wen, A. Kang, Z. Gui, L. Li, Phase transitions in nanocrystalline barium titanate ceramics prepared by spark plasma sintering. J. Am. Ceram. Soc. **89–3**, 1059–1064 (2006)
10. S. Ammar, A. Helfen, N. Jouini, F. Fiévet, I. Rosenman, F. Villain, P. Molinié, M. Danot, Magnetic properties of ultrafine cobalt ferrite particles synthesised by hydrolysis in a polyol medium. J. Mater. Chem. **11**, 186–192 (2001)
11. L. Lutterotti, S. Matthies and H. R. Wenk, MAUD: a friendly Java program for material analysis using diffraction, IUCr: Newsletter of the CPD 21 (1999), pp. 14–15
12. S. Aoyagi, Y. Kuroiwa, A. Sawada, H. Kawaji, T. Atake, Size effect on crystal structure and chemical bonding nature in $BaTiO_3$ nanopowder. J. Therm. Anal. Calorim. **81**, 627–630 (2005)
13. A. Tokeer, K. Gnanasundaram, N. Chandrabhas, A.K. Ganguli, Nanostructured barium titanate prepared through a modified reverse micellar route: structural distortion and dielectric properties. J. Mater. Res. **20**, 1415–1421 (2005)
14. J.Q. Qi, T. Peng, Y.M. Hu, Direct synthesis of ultrafine tetragonal $BaTiO_3$ nanoparticles at room temperature. Nanoscale Res. Lett. **6**, 466–467 (2011)
15. M.B. Smith, K. Page, T. Siegrist, P.L. Redmond, E.C. Walter, R. Seshadri, L.E. Brus, M.L. Steigerwald, Crystal structure and the paraelectric-to-ferroelectric phase transition of nanoscale $BaTiO_3$. J. Am. Chem. Soc. **130**, 6955–6963 (2008)
16. M. El Marssi, F. Le Marrec, I.A. Lukyanchuk, M.G. Karkut, Ferroelectric transition in an epitaxial barium titanate thin film: Raman spectroscopy and x-ray diffraction study. J. Appl. Phys. **94**, 3307–3312 (2003)
17. S. Wada, T. Suzuki, M. Osada, M. Kakihana, T. Noma, Change of macroscopic and microscopic symmetry of barium titanate single crystal around curie temperature. Jpn. J. Appl. Phys. **37**, 5385–5393 (1998)
18. S. Yoon, J. Dornseiffer, Y. Xiong, D. Grüner, Z. Shen, S. Iwaya, C. Pithan, R. Waser, Spark plasma sintering of nanocrystalline $BaTiO_3$-powders: consolidation behavior and dielectric characteristics. J. Eur. Cer. Soc. **31**, 1723–1731 (2011)
19. N. Hirose, A.R. West, Impedance spectroscopy of undoped $BaTiO_3$ ceramics. J. Am. Ceram. Soc. **79**, 1633–1641 (1996)